Single-photon frequency-comb generation in a one-dimensional waveguide coupled to two atomic arrays

Zeyang Liao,[1,*] Hyunchul Nha,[2] and M. Suhail Zubairy[1,†]
[1]*Institute for Quantum Science and Engineering (IQSE) and Department of Physics and Astronomy, Texas A&M University, College Station, Texas 77843-4242, USA*
[2]*Department of Physics, Texas A&M University at Qatar, Education City, P.O. Box 23874, Doha, Qatar*
(Received 21 December 2015; revised manuscript received 9 February 2016; published 28 March 2016)

An atomic chain coupled to a one-dimensional (1D) photonic waveguide can become a very good atom mirror. This atom mirror can have a very high reflectivity for a single-photon pulse due to the collective interaction between the atoms. Two atom arrays coupled to a 1D waveguide can form a good cavity. When a single-photon pulse is incident from one side of the cavity, only a discrete subset of photon frequencies can transmit the cavity and the transmitted frequencies are almost equally spaced, which is similar to a frequency comb. The linewidth of the comb frequency can be reduced if we increase the atom number in the atomic arrays. More interestingly, if the photon pulse is initially inside the cavity, the photon spectrum after a long time of interaction is also discretized with the comb frequencies being significantly amplified while other frequencies being largely suppressed. This single-photon frequency comb may be useful for precision measurement.

DOI: 10.1103/PhysRevA.93.033851

I. INTRODUCTION

Due to the fact that photons are an ideal carrier of quantum information, manipulating and routing photons can have very important applications in quantum information and quantum computation [1–5]. Waveguide QED is an extremely promising candidate for this purpose because it cannot only enhance the atom-photon interaction due to the Purcell effect [6] but also guide the photons [7,8]. Indeed, a number of possible applications have been proposed, such as a single-photon diode [9,10], efficient single-photon frequency conversion [11–14], single-photon transistor [15,16], a single-photon quantum router with multiple output ports [17], and a two-photon control phase gate in a 1D waveguide [18,19]. A number of systems may serve as very good 1D waveguides, such as optical nanofibers [20], photonic crystal with line defects [21], surface plasmon nanowire [22], and superconducting microwave transmission lines [23–27].

A single or few photons scattered by an emitter or multiple atoms coupled to a 1D waveguide has been widely studied both in theory [28–43] and experiment [44–49]. It is found that a photon with frequency resonant with a two-level atom can be reflected with high probability. Indeed, 94% extinction of the transmitted photon has been observed experimentally in the circuit QED system [50]. The reflectivity can be further enhanced by the collective effect of multiple atoms and the system can act as a very good mirror [51,52]. Two arrays of atoms coupled to a 1D waveguide can then become a very good cavity. An atom placed within this cavity can be strongly coupled with the photons stored in this cavity and the vacuum Rabi splitting can occur [52]. It has also been shown that quantum information may be stored in this cavity.

In 2015 we derived a time-dependent dynamical theory for studying how a single photon propagates through an atomic chain coupled to a 1D waveguide [43], where we show that many interesting physics can occur in this system such as the photonic band gap effects [28], long-range quantum entanglement generation [53,54], Fano-like interference [55–58], and super-radiant effects [59,60]. In this paper we employ this dynamical theory to study how a single photon being scattered by the cavity formed by two atom arrays coupled to a 1D waveguide. We show that the photon spectrum can be strongly modified and a single-photon frequency comb can be generated. Here we study two cases: In the first case the single photon is incident from outside of the cavity where we show that only discretized frequency components can transmit through the system. In the second case the single photon is initially in the cavity where we show that it can be reflected back and forth inside the cavity and photon mode conversion can occur with some discretized frequency components being significantly enhanced. In both cases, a single-photon frequency comb may be generated.

A frequency comb is a light with a series of discrete, equally spaced spectrum [61]. Optical frequency combs provide equidistant frequency markers over a large frequency range and they can be used to link an unknown optical frequency to a more accurate radio or microwave frequency reference. It has been widely used in optical frequency metrology and precision measurements. It can be generated by a number of mechanisms, including amplitude modulation (AM) of a continuous wave laser [62], stabilization of the pulse train generated by a mode locked laser [63], or by the interaction between a continuous-wave pump laser of a known frequency with the modes of a monolithic ultra-high-Q microresonator via the Kerr nonlinearity [64–66]. In addition to the traditional optical frequency comb with a huge number of photons, a single-photon frequency comb is also interesting because it can simultaneously suppress the uncertainties of time and energy [67]. One advantage of our method to generate a single-photon frequency comb via the waveguide-QED system is that the frequency-comb photon can be confined and guided by the waveguide which is good for manipulation. In addition, different from the traditional case based on a

*zeyangliao@physics.tamu.edu
†zubairy@physics.tamu.edu

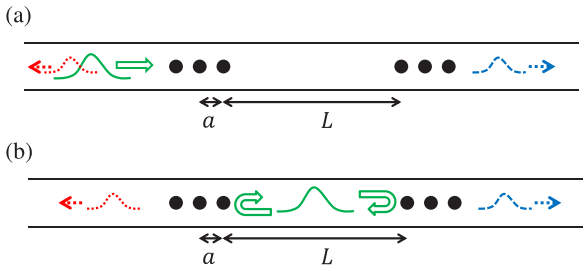

FIG. 1. Single-photon transport through a linear atomic chain coupled to a one-dimensional photonic waveguide. (a) A single photon is incident from the left of the atomic cavity. (b) A single photon is initially inside the atomic cavity.

high-Q resonator, the atomic array here plays the roles of both the gain medium and the resonator. In our method the other frequency components can be converted to the comb frequency components by the coherent nonlinear interactions which may provide a higher efficiency to generate a single-photon frequency comb.

This paper is organized as follows. In Sec. II we show our model and illustrate how to calculate the photon spectra for a single-photon transport in a 1D waveguide coupled to two atomic arrays. In Sec. III we present the results when the single photon is incident from one side of the atomic cavity. In Sec. IV we present the results when the single photon is initially inside the atomic cavity. In Sec. V we discuss the effects of the decay to the nonguided modes. Finally, we summarize the results.

II. MODEL AND THEORY

The models we study are shown in Fig. 1. Two atomic arrays are coupled to a 1D photonic waveguide and they are separated by a distance L. Each atom is considered as a two-level system with transition frequency ω_a. The atoms in each array are separated by $\lambda/2$ with λ being the wavelength corresponding to the transition frequency of the two-level atom. All the atoms are initially in the ground state. This setup can become a cavity where photons can be reflected back and forth by the two atom mirrors. In this paper we study two cases: (a) a single-photon pulse is incident from the left side of the cavity [Fig. 1(a)]; and (b) a single-photon pulse is initially inside the cavity [Fig. 1(b)].

The Hamiltonian of the system in the rotating wave approximation is given by [43,68]

$$H = \frac{\hbar}{2}\left(\omega_a - i\frac{\gamma}{2}\right)\sum_{j=1}^{N}\sigma_j^z + \hbar\sum_k \omega_k a_k^\dagger a_k + \hbar\sum_{j=1}^{N}\sum_k (g_k e^{ikr_j} a_k \sigma_j^+ + g_k^* e^{-ikr_j} a_k^\dagger \sigma_j^-), \quad (1)$$

where the first term is the atomic energy, the second term is the energy of the guided photon mode, and the third term is the coupling between the atoms and the guided photon modes. Here N is the number of atoms coupled to the 1D waveguide, r_j is the position of the jth atom, $\sigma_j^+ = |e\rangle_j\langle g|(\sigma_j^- = |g\rangle_j\langle e|)$ is the raising (lowering) operator of the jth atom, ω_k is the angular frequency of the photon with wave vector k, $a_k^\dagger(a_k^-)$ is the corresponding creation (annihilation) operator, and g_k is the coupling strength between the atoms and a guided photon with wave vector k. Assuming that ω_a is far away from the cutoff frequency of the photonic waveguide and the photon spectrum is narrow, the dispersion relation for the guided photon can be approximately linearized as $\omega_k = \omega_a + (|k| - k_a)v_g$, where k_a is the wave vector at frequency ω_a and v_g is the group velocity [69].

For a single-photon excitation, the quantum state of the system in arbitrary time can be written as

$$|\Psi(t)\rangle = \sum_{j=1}^{N}\alpha_j(t)e^{-i\omega_a t}|e_j,0\rangle + \sum_k \beta_k(t)e^{-i\omega_k t}|g,1_k\rangle \quad (2)$$

in which $|e_j,0\rangle$ is the state when only the jth atom is excited with zero photon being in the waveguide and $\alpha_j(t)$ is the corresponding amplitude, $|g,1_k\rangle$ is the state when all the atoms are in the ground state with one photon with wave vector k being in the waveguide, and $\beta_k(t)$ is the corresponding amplitude. From the Schrödinger equation and by integrating out the photon parts (see the Appendix or Ref. [43] for derivation), one can obtain the dynamics of the atomic system which is given by

$$\dot{\alpha}_j(t) = b_j(t) - \frac{1}{2}\sum_{l=1}^{N}(\Gamma e^{ik_a r_{jl}} + \gamma\delta_{jl})\alpha_l\left(t - \frac{r_{jl}}{v_g}\right), \quad (3)$$

where the first term in the right-hand side

$$b_j(t) = -\frac{i}{2\pi}\sqrt{\frac{\Gamma v_g L_q}{2}}\int_{-\infty}^{\infty}\beta_k(0)e^{ikr_j - i\delta\omega_k t}dk \quad (4)$$

is the excitation by the incident photon with spectrum $\beta_k(0)$, $\Gamma = 2L_q|g_{k_a}|^2/v_g$ is the coupling strength between the atom and the guided photon with L_q being the quantization length of the guided modes, and $r_{jl} = |r_j - r_l|$. The second term includes the collective interaction between the atoms and the spontaneous decay to the nonguided modes. Different from the case in the free space, the collective interactions induced by the guided photon are a long-range effect. When the atomic separation is much smaller than the size of the photon wave packet, the time-retarded effect can be neglected which is the usual Markovian approximation. However, when the atomic separation is comparable to the the size of the photon wave packet, the time-retarded factor should be considered. Since the separation between the two atom arrays is comparable to the photon wave packet, here we cannot neglect the time-retarded effect.

The photon spectrum in arbitrary time can be calculated by Eq. (A3) in the Appendix. Assuming that the single-photon pulse is initially propagating right, we have the left propagating modes at time t given by

$$\beta_{\delta k}^L(t) = -i\sqrt{\frac{\Gamma v_g}{2L}}\sum_{j=1}^{N_a}e^{i(k_a+\delta k)r_j}\int_0^t \alpha_j(t')e^{i\delta k v_g t'}dt', \quad (5)$$

where $\delta k = |k| - k_a$ with $k < 0$. On the other hand, for the right propagating modes we have

$$\beta^R_{\delta k}(t) = \beta_k(0) - i\sqrt{\frac{\Gamma v_g}{2L}}\sum_{j=1}^{N_a} e^{-i(k_a+\delta k)r_j}\int_0^t \alpha_j(t')e^{i\delta k v_g t'}dt', \tag{6}$$

where $\delta k = k - k_a$ with $k > 0$.

For $t \to \infty$, the photon spectra for the left and right propagating field are respectively given by [43]

$$\beta^L_{\delta k}(t\to\infty) = -i\sqrt{\frac{\Gamma v_g}{2L_q}}\sum_{j=1}^{N} e^{i(k_a+\delta k)r_j}\chi_j(\delta k), \tag{7}$$

$$\beta^R_{\delta k}(t\to\infty) = \beta_{\delta k}(0) - i\sqrt{\frac{\Gamma v_g}{2L_q}}\sum_{j=1}^{N} e^{-i(k_a+\delta k)r_j}\chi_j(\delta k), \tag{8}$$

where we assume that the photon is propagating to the right and $\chi_j(\delta k) = \int_{-\infty}^{\infty}\alpha_j(t)e^{i\delta k v_g t}dt$ which is given by

$$\chi_j(\delta k) = \sum_{l=1}^{N} M^{-1}_{jl}(\delta k)B_l(\delta k), \tag{9}$$

with $M(\delta k) = V_N(\delta k) + (\gamma/2 - i\delta k v_g)I_N$, where I_N is a $N\times N$ unit matrix and $V_N(\delta k)$ is given by

$$V_N(\delta k) = \frac{\Gamma}{2}\begin{bmatrix} 1 & e^{ikr_{12}} & \cdots & e^{ikr_{1N}} \\ e^{ikr_{21}} & 1 & \cdots & e^{ikr_{2N}} \\ \vdots & \vdots & \ddots & \vdots \\ e^{ikr_{N1}} & e^{ikr_{N2}} & \cdots & 1 \end{bmatrix} \tag{10}$$

and $B_j(\delta k) = -i\sqrt{\Gamma L_q/2v_g}\beta_{\delta k}(0)e^{i(k_a+\delta k)r_j}$. The photon pulse shapes can also be calculated by performing the Fourier transformations on the photon spectra shown in Eqs. (5) and (6) and they are given by

$$\beta^L_x(t) = e^{-ik_a x}\int_{-\infty}^{\infty}\beta^L_{\delta k}(t)e^{-i\delta k(x+v_g t)}d\delta k, \tag{11}$$

$$\beta^R_x(t) = e^{ik_a x}\int_{-\infty}^{\infty}\beta^R_{\delta k}(t)e^{i\delta k(x-v_g t)}d\delta k. \tag{12}$$

In the following sections we fist present the results when the decay to the nonguided modes is neglected and the results when the effect of the decay to the nonguided modes is included are discussed in Sec. V.

III. CASE I: PHOTON IS INCIDENT FROM ONE SIDE OF THE ATOMIC CAVITY

In the first case, the single-photon pulse is assumed to be incident from the left of the atomic cavity. All through this paper we assume that the incident photon has a Gaussian shape and its spectrum is given by

$$\beta_{\delta k}(0) = \frac{(8\pi)^{1/4}}{\sqrt{\Delta L_q}}e^{-\frac{\delta k^2}{\Delta^2}}, \tag{13}$$

where Δ is the width in the k space with the full width at half maximum of the spectrum being $\sqrt{2\ln 2}\Delta v_g$. In the following, we calculate the spectrum and the photon pulse shape after the scattering by the atomic cavity shown in Fig. 1(a). In this section we first neglect the effect of the decay to the nonguided modes (i.e., $\gamma = 0$). The results when $\gamma \neq 0$ are discussed in Sec. V.

For the simplest case when there are only two atoms with separation being L, the reflected and transmitted photon spectrum when $t \to \infty$ can be calculated to be

$$\left|\beta^L_{\delta k}\right|^2 = |\beta_{\delta k}(0)|^2\frac{4(\sin kL + \eta_{\delta k}\cos kL)^2}{\eta^4_{\delta k} + 4[\sin kL + \eta_{\delta k}\cos kL]^2}, \tag{14}$$

$$\left|\beta^R_{\delta k}\right|^2 = |\beta_{\delta k}(0)|^2\frac{\eta^4_{\delta k}}{\eta^4_{\delta k} + 4[\sin kL + \eta_{\delta k}\cos kL]^2}, \tag{15}$$

where $k = k_a + \delta k, \eta_{\delta k} = 2\delta k v_g/\Gamma$. It is readily seen that $|\beta^R_{\delta k}|^2 + |\beta^L_{\delta k}|^2 = |\beta_{\delta k}(0)|^2$, which indicates that the photon modes are conserved in this case, i.e., a photon with wave vector k can be either reflected or transmit but not be converted to other modes. The result when $\Gamma = \Delta v_g, \Delta = 0.01k_a$, and $L = 200\lambda$ is shown in Fig. 2(a) where the black solid line is the incident photon spectrum, the red dotted line is the reflected photon spectrum, and the blue dashed line is the transmitted photon spectrum. It is noted that only a discrete subset of frequencies can be transmitted in this atom cavity which is similar to a frequency comb. Since only one photon is involved here, it may be termed as "single-photon frequency comb." Here we have two complimentary single-photon frequency combs because the reflected photon and the transmitted photon are complimentary to each other.

The peak positions are determined by the condition $\tan(k_a + \delta k)L = -2\delta k v_g/\Gamma$. For the current example we have $k_a L = 400\pi$. The condition for the peak positions becomes $\tan(\delta k L) = -2\delta k v_g/\Gamma$. If $\delta k v_g/\Gamma \ll 1$, the peak positions are approximately given by $\delta k_n = n\pi/(L + 2v_g/\Gamma)$ with $n = \pm1, \pm2, \ldots$ being the index of the comb frequency. The spacing between the comb frequency is then given by $\pi/(L + 2v_g/\Gamma)$ with an effective cavity length being $L_{\text{eff}} \simeq L + 2v_g/\Gamma$. The linewidth can be calculated to be $(1/F)(\pi/L_{\text{eff}})$, where $F = L^2_{\text{eff}}\Gamma^2/(8n^2\pi v_g^2)$ is the finesse of the atom cavity. It is noted that the linewidth depends on the comb frequency index n. The comb line with larger n has broader linewidth which can also be seen from Fig. 2(a). In the current example, the effective cavity length $L_{\text{eff}} \simeq 232\lambda$, and the comb frequency line spacing is about 0.22Δ. The finesse $F \simeq 8.45/n^2$. For $n = 1, F \simeq 8.45$ and the linewidth is about 0.02Δ. However, when $n = 3, F \simeq 0.9$ and the linewidth is about 0.22Δ, which is about the line spacing. Therefore, the comb lines for larger n can overlap with each other which can also be clearly seen from Fig. 2(a). One should note that for larger n when $\delta k_n v_g/\Gamma \sim 1$, the effective cavity length and the finesse can significantly deviate from the calculations above. It is also noted that the center frequency is completely reflected back.

The photon pulse after the interactions is shown in Fig. 2(c). The photon has a large probability to be reflected back at the first time when the incident photon interacts with the atomic array. The photon entering the atomic cavity can be reflected back and forth and pulses can be generated with each pulse being three peaks. The reason why there are three peaks can be explained by the interference between the incident photon pulse and the re-emitted photon pulses by the two atomic arrays. We can also see that the pulse amplitude decays quickly

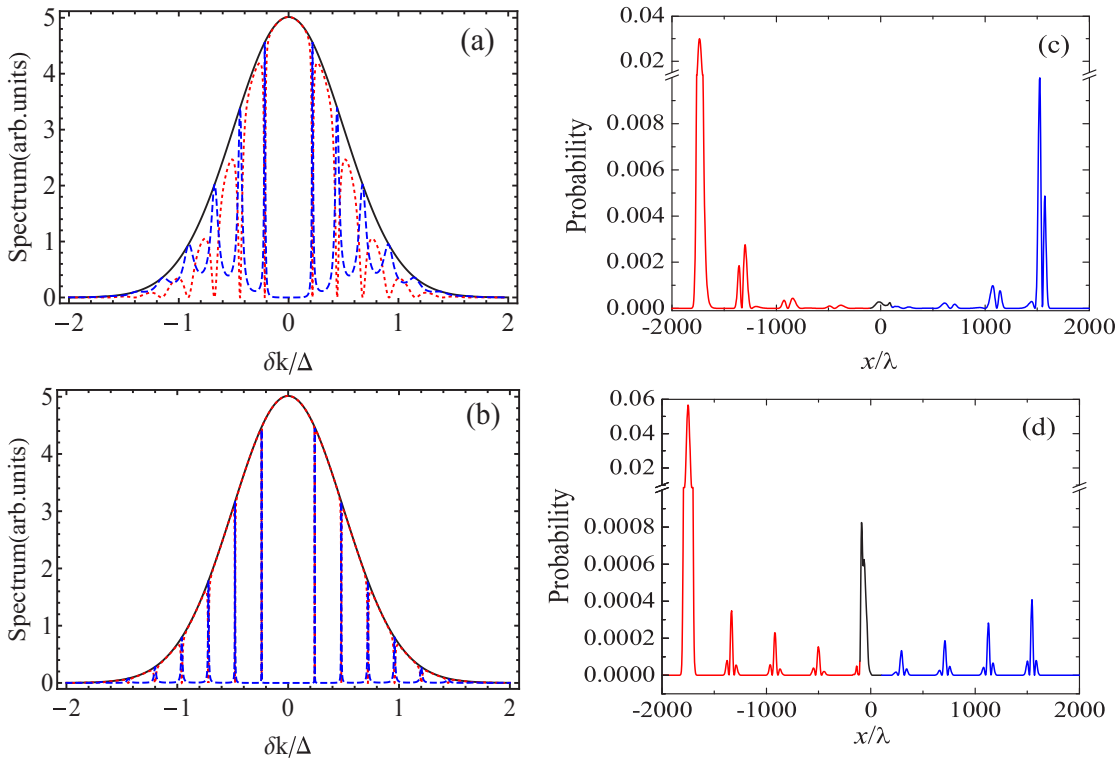

FIG. 2. The results when the photon is incident from one side of the cavity. (a) and (b) The spectrum of incoming photon before the interaction (black solid line), left (red dotted line) and right (blue dashed line) propagating photon after the interaction. (c) and (d) The pulses propagating to the left (red solid line), to the right (blue solid line), and the pulse in the atomic cavity at time $t = 120/\Gamma$ where we assume that the pulse is initially $10/\Delta$ away from the left side of the atomic cavity. (a) and (c) The results of the two-atom cavity. (b) and (d) The results of the eight-atom cavity. Parameter: $\Gamma = \Delta v_g$ and $\Delta = 0.01k_a$.

in this case. The interval between each pulse is related to the spacing of the frequency comb.

The single-photon frequency comb shown in Fig. 2(a) is not a very good comb because the line spacing is not very uniform. One way to improve the quality of the comb is by increasing the atom number in each array. The reflection and transmission spectra for an arbitrary atom number can be calculated by Eqs. (7) and (8). One example when there are four atoms on each array is shown in Fig. 2(b). Similar to the two-atom case, two complimentary single-photon frequency combs are also generated here. However, due to the collective enhanced coupling, the reflectivity of the atom cavity is significantly increased and therefore the decay rate of the photon amplitude inside the atomic cavity is largely reduced which leads to a much narrower linewidth of the single-photon frequency. The comb line spacing is also much more uniform. Actually, the spectrum calculated by Eqs. (7) and (8) for N atoms can be well approximated by Eqs. (14) and (15) with Γ being replaced by $N\Gamma/2$ [59,70]. Thus we have $\eta_{\delta k} \to \eta'_{\delta k} = 4\delta k v_g/(N\Gamma)$. When $\eta'_{\delta k} \ll 1$, the effective cavity length is given by $L'_{\rm eff} \simeq L + (4v_g/N\Gamma)$ and the comb line spacing is given by $\pi/L'_{\rm eff}$. For large N, the condition $\eta'_{\delta k} \ll 1$ can hold for all the frequencies within the incident photon bandwidth. Hence the line spacings can be uniform and given by $\pi/L'_{\rm eff}$. The effective cavity length can approach L when $N \to \infty$. The linewidth is then given by $(1/F)(\pi/L_{\rm eff})$ with $F = L'^2_{\rm eff}N^2\Gamma^2/(32n^2\pi v_g^2)$. Therefore, the linewidth can also be reduced by increasing the atom number. In the current example with $N = 8$, the effective cavity length $L_{\rm eff} \simeq 208\lambda$ and the comb line spacing is about 0.2Δ. The finesse $F = 108.7/n^2$. When $n = 1, F = 108.7$ and the linewidth is about 0.0018Δ. When $n = 3, F = 12.1$ and the linewidth is about 0.016Δ, which is still much smaller than the comb line spacing. Therefore, the comb lines do not overlap in this case. The photon pulses after the interaction are shown in Fig. 2(d). Similar to the two-atom case, most of the energy is reflected back and the transmitting photon is a pulse chain with each pulse being three peaks. We can see that the number of peaks in each pulse does not depend on how many atoms in each atomic array. We note that the first reflected pulse in Fig. 2(d) is larger than that in Fig. 2(c). This is because the reflectivity of the atomic array with a larger atom number is higher than that with a smaller atom number. Therefore, the incoming photon has a larger probability to be directly reflected back with a larger atom number. However, with a larger number of atoms the photon entering into the cavity has a lower probability to be leaked out which results in a smaller decay rate in the photon amplitude of the following pulse chain [Fig. 2(d)] and therefore narrower linewidth in the spectrum [Fig. 2(b)].

If $N \to \infty$, a perfect single-photon frequency comb may be formed with line spacing being π/L and linewidth being infinitely small. However, when $N \to \infty$, the transmission probability approaches zero, i.e., the photon is completely reflected back. Hence, the probability to detect a single-photon frequency comb is zero. In the next section we show that the amplitude of the comb line can be largely enhanced

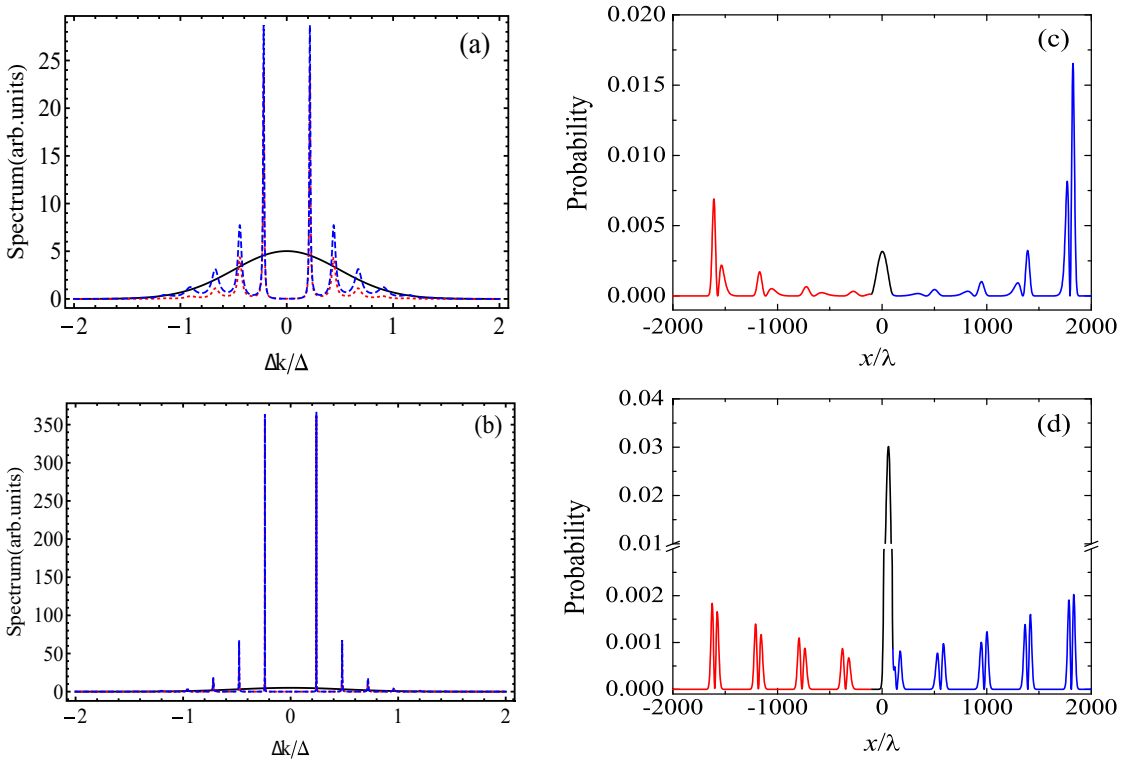

FIG. 3. The results when the photon is initially inside the cavity. (a) and (b) The spectrum of incoming photon before the interaction (black solid line), left (red dotted line) and right (blue dashed line) propagating photon after the interaction. (c) and (d) The pulses propagating to the left (red solid line), to the right (blue solid line), and the pulse in the atomic cavity at time $t = 120/\Gamma$ where we assume that the pulse is initially at the center of the atomic cavity. (a) and (c) The results of the two-atom cavity. (b) and (d) The results of the eight-atom cavity. Parameter: $\Gamma = \Delta v_g$ and $\Delta = 0.01 k_a$.

if the single-photon pulse is initially inside of the atomic cavity.

IV. CASE II: PHOTON IS INITIALLY INSIDE THE ATOMIC CAVITY

In this section we consider the case when the single-photon pulse is initially in the center of the atom cavity. This may be achieved by the following procedures. Supposing that a single-photon pulse is propagating from the left, we first turn on an external electric or magnetic field to modify the energy of the atoms on the left array such that the frequency of the photon is largely detuned from the transition frequency of the atom. Due to the energy mismatch, the photon can propagate through the left atomic array without being scattered. After that we turn off the external field and the photon can then be trapped inside the atom cavity. In this case we also compare the results of two-atom and eight-atom cavities. Also, we first neglect the effect of the decay to the nonguided modes (i.e., $\gamma = 0$) in this section.

For the two-atom cavity, the photon spectra after a long time of interaction can be calculated by Eqs. (7)–(10) with $B_l(\delta k) = 0$ for the atom on the left and they are given by

$$|\beta_{\delta k,L}|^2 = |\beta_{\delta k}(0)|^2 \frac{\eta_{\delta k}^2}{\eta_{\delta k}^4 + 4[\sin kL + \eta_{\delta k}\cos kL]^2}, \quad (16)$$

$$|\beta_{\delta k,R}|^2 = |\beta_{\delta k}(0)|^2 \frac{\eta_{\delta k}^2\left(1+\eta_{\delta k}^2\right)}{\eta_{\delta k}^4 + 4[\sin kL + \eta_{\delta k}\cos kL]^2}. \quad (17)$$

where $k = k_a + \delta k, \eta_{\delta k} = 2\delta k v_g/\Gamma$. We have

$$|\beta_{\delta k,L}|^2 + |\beta_{\delta k,R}|^2 = |\beta_{\delta k}(0)|^2 \frac{2\eta_{\delta k}^2 + \eta_{\delta k}^4}{\eta_{\delta k}^4 + 4(\sin kL + \eta_{\delta k}\cos kL)^2}, \quad (18)$$

which is usually not equal to $|\beta_{\delta k}(0)|^2$. Hence, different from the first case shown in the previous section, the mode conversion can occur in the current setup. When $\eta_{\delta k}^2 > 2(\sin kL + \eta_{\delta k}\cos kL)^2$, the mode is enhanced. On the contrary, when $\eta_{\delta k}^2 < 2(\sin kL + \eta_{\delta k}\cos kL)^2$, the mode is suppressed.

For numerical results we also assume that the photon pulse has a Gaussian shape as shown in Eq. (13) with $\Gamma = \Delta v_g$ and $\Delta = 0.01 k_a$. The results when there are two atoms with separation $L = 200\lambda$ are shown in Figs. 3(a) and 3(c). Similar to the previous cases, two frequency combs can be generated with one propagating to the left and the other propagating to the right. However, different from the previous cases, the amplitudes of the comb lines here are significantly enhanced and the other frequencies are largely suppressed. The nonlinear frequency conversion can occur in this system. Another difference is that two similar frequency combs instead of two complimentary frequency combs are generated here. Similar to case I, when $\eta_{\delta k} \ll 1$, the comb line spacing is about π/L_{eff} with $L_{\text{eff}} \simeq L + (2v_g/\Gamma)$ and the linewidth is given by $(1/F)(\pi/L_{\text{eff}})$ with $F = L_{\text{eff}}^2\Gamma^2/(8n^2\pi v_g^2)$. The comb frequency away from the center frequency has a broader linewidth due to the fact that the reflectivity for these

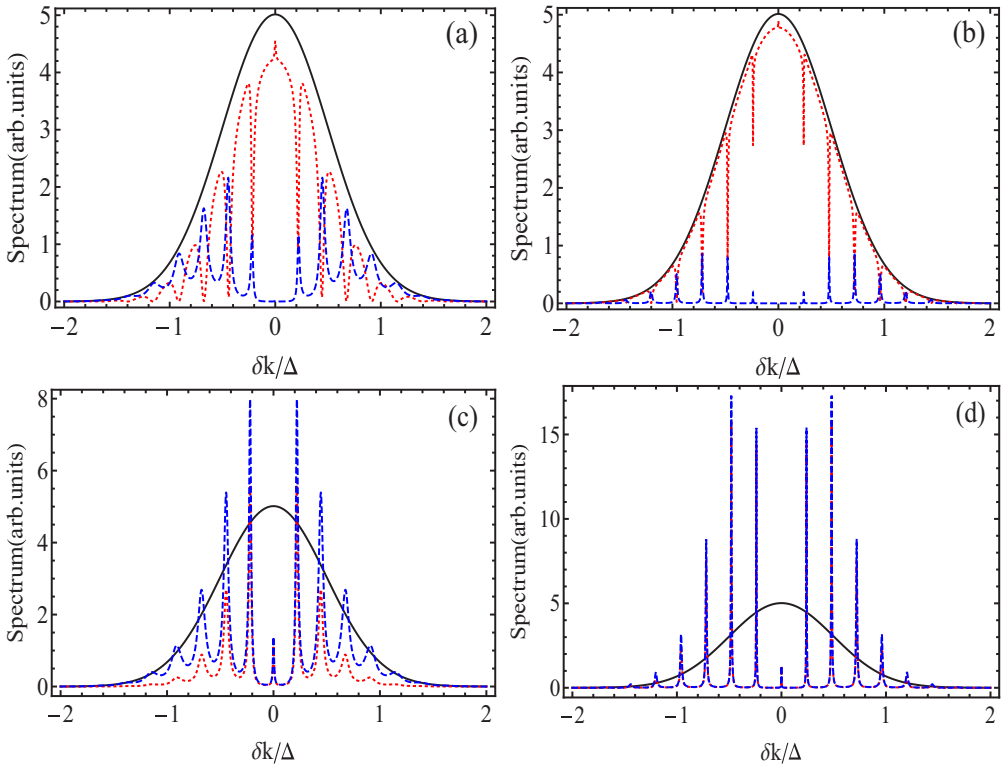

FIG. 4. The spectrum of the incoming, reflection, and transmission photon. (a) and (b) The incoming photon is initially outside the cavity with (a) being the results when there are two atoms and (b) being the results when there are eight atoms. (c) and (d) The incoming photon is initially inside the cavity with (a) being the results when there are two atoms and (b) being the results when there are eight atoms. Parameter: $\Gamma = \Delta v_g, \Delta = 0.01k_a$, and $\gamma = \Gamma/10$.

frequencies are smaller. In the current example, $L_{\rm eff} \simeq 232\lambda$ and $F \simeq 8.45/n^2$. The line spacing is about 0.22Δ and the linewidth is about 0.02Δ. For $n = 1$, the comb frequency is given by $\delta k_1 = \pi/L_{\rm eff} \simeq 0.22\Delta$ and this frequency component is enhanced by a factor $1/\eta^2_{(\pi/L_{\rm eff})} \simeq 5.4$. The photon pulses are shown in Fig. 3(c) where one sees that the photon is periodically leaking out of the cavity. There are two peaks in each pulse due to the interference between the initial photon pulse and the re-emitted photon by the atom on the right. We can see that the pulse amplitude decreases with time quickly due to the lower reflectivity.

When we increase the atom number such that there are four atoms on each side, the photon spectrum can also be calculated by Eqs. (7)–(10) with $B_l(\delta k) = 0$ for all the atoms on the left (i.e., $j = 1, \ldots, 4$). The spectra are shown in Fig. 3(b) where we can see that the comb frequency is enhanced even larger and the linewidth of the comb frequency is also much narrower. In fact, the spectra for multiple-atom arrays can be well approximated by replacing $\eta_{\delta k}$ in Eqs. (16) and (17) by $2\eta_{\delta k}/N$ with N being the total number of atoms. Similar to case I, when $2\eta_{\delta k}/N \ll 1$, the comb line spacing is about $\pi/L_{\rm eff}$ with $L'_{\rm eff} \simeq L + (4v_g/N\Gamma)$ and the linewidth is given by $(1/F)(\pi/L'_{\rm eff})$ with $F = L'^2_{\rm eff}N^2\Gamma^2/(32n^2\pi v_g^2)$. The comb frequency away from the center frequency has a broader linewidth due to the fact that the reflectivity for these frequencies are smaller. However, different from case I, the comb frequencies are significantly enhanced. In the current example with $N = 8, L_{\rm eff} \simeq 208\lambda$ and $F \simeq 108.7/n^2$. For $n = 1$, the comb frequency is given by $\delta k_1 = \pi/L'_{\rm eff}$ and this frequency is enhanced by a factor $N^2/4\eta^2_{\pi/L'_{\rm eff}} \simeq 69$. The photon pulses after the scattering are shown in Fig. 3(d) where we see that each pulse has also two peaks which is similar to the two-atom case. However, the pulse amplitude decreases much slower than that of the two-atom case which can result in a narrower linewidth in the spectrum.

V. THE EFFECTS OF DECAY TO THE NONGUIDED MODES

In the previous sections the decay to the nonguided modes has been neglected. In this section we would study how the spectrum is changed if the decay to the nonguided modes is included.

For the case when the single-photon pulse is incident from outside of the atomic cavity, the reflection and transmission spectra when there are only two atoms are respectively given by

$$\left|\beta^L_{\delta k}\right|^2 = |\beta_{\delta k}(0)|^2 \left| \frac{\eta_\Gamma(1+e^{2ika})(1-i\eta_{\delta k}) - 2\eta^2_\Gamma e^{2ika}}{(1-i\eta_{\delta k})^2 - \eta^2_\Gamma e^{2ika}} \right|^2, \quad (19)$$

$$\left|\beta^R_{\delta k}\right|^2 = |\beta_{\delta k}(0)|^2 \left| \frac{(1-\eta_\Gamma - i\eta_{\delta k})^2}{(1-i\eta_{\delta k})^2 - \eta^2_\Gamma e^{2ika}} \right|^2, \quad (20)$$

where $\eta_\Gamma = \Gamma/(\Gamma+\gamma)$ and $\eta_{\delta k} = 2\delta k v_g/(\Gamma+\gamma)$. When $\gamma = 0$, Eqs. (19) and (20) are reduced to Eqs. (14) and (15). A typical result is shown in Fig. 4(a), where the parameters are the same as those used in Fig. 2(a) with $\gamma = \Gamma/10$. Similar

to Fig. 2(a), the comb structure is generated. However, the amplitude here is reduced due to the loss to the nonguided modes. When the number of atoms is increased, the spectra can be well approximated by Eqs. (19) and (20) with $\Gamma \to N\Gamma/2$, where N is the number of atoms. The results when there are four atoms on each side and the parameters are the same as those used in Fig. 2(b) with $\gamma = \Gamma/10$ are shown in Fig. 4(b) where we see that the spectrum has a narrower linewidth comparing with the results when there are only two atoms.

For the case when the single-photon pulse is initially inside the atomic cavity, the reflection and transmission spectra when there are only two atoms are respectively given by

$$\left|\beta_{\delta k}^{L}\right|^2 = |\beta_{\delta k}(0)|^2 \left| \frac{\eta_\Gamma^2 - \eta_\Gamma(1 - i\eta_{\delta k})}{(1 - i\eta_{\delta k})^2 - \eta_\Gamma^2 e^{2ika}} \right|^2, \tag{21}$$

$$\left|\beta_{\delta k}^{R}\right|^2 = |\beta_{\delta k}(0)|^2 \left| \frac{(1 - i\eta_{\delta k})(1 - \eta_\Gamma - i\eta_{\delta k})}{(1 - i\eta_{\delta k})^2 - \eta_\Gamma^2 e^{2ika}} \right|^2, \tag{22}$$

where $\eta_\Gamma = \Gamma/(\Gamma + \gamma)$ and $\eta_{\delta k} = 2\delta k v_g/(\Gamma + \gamma)$. When $\gamma = 0$, Eqs. (21) and (22) are reduced to Eqs. (16) and (17). Similar to previous cases, when we increase the number of atoms, the spectra can be well approximated by Eqs. (21) and (22) with Γ being replaced by $N\Gamma/2$. The results when there are two atoms and eight atoms are respectively shown in Figs. 4(c) and 4(d) where we see that comb structures can be generated and the comb lines can be significantly enhanced. However, due to the leakage to the nonguided modes, the enhanced factors are reduced. Therefore, provided that the decay to the nonguided modes is not very large, the single-photon frequency comb can also be generated even if the decay to the nonguided modes is included.

VI. SUMMARY

In summary, we studied how a single-photon pulse interacts with a cavity formed by two atomic arrays. Due to the collective enhanced coupling, the atomic array coupled to a 1D waveguide can have a very high reflectivity and the finesse of the cavity formed by the two atom arrays can increase with the atom number. A single-photon pulse can be stored in this cavity for an extended period of time which may be used as a single-photon storage. More interestingly, the photon spectrum after a long time of interaction can be discretized and a single-photon frequency comb can be generated. When the single-photon pulse is initially in the atom cavity, nonlinear frequency conversion can occur and the comb frequency can be largely enhanced while other frequencies are largely suppressed. The single-photon frequency comb can also be generated even if the decay to the nonguided modes is not very large compared with the coupling to the guided modes.

This system may find applications in precision measurement. Since the line spacing between the comb frequencies depends on the atomic distance and the line spacing of the frequency comb can be measured with high precision by the radio or microwave frequency reference, the setup here may provide a way to determine the atomic separation L with high accuracy. The linewidth of the frequency comb can introduce an uncertainty when we measure the line spacing. Therefore, the narrower the linewidth, the less uncertainty we have. Our frequency may also be used as a frequency ruler. However, to become a frequency ruler, we have to calibrate the frequency comb precisely which usually requires that the frequency comb can span an octave. In future study, we shall study how to extend our comb frequency to an octave. If we can achieve that, our frequency comb may also be able to link an unknown optical frequency to a more accurate radio or microwave frequency reference.

ACKNOWLEDGMENT

This work is supported by a grant from the Qatar National Research Fund (QNRF) under the NPRP project 7-210-1-032.

APPENDIX

From the Schrödinger equation $i\hbar\partial_t|\Psi(t)\rangle = H|\Psi(t)\rangle$ with H being given by Eq. (1) and $|\Psi(t)\rangle$ being given by Eq. (2), we have the following dynamic equations:

$$\dot{\alpha}_j(t) = -i\sum_k g_k e^{ikr_j}\beta_k(t)e^{-i\delta\omega_k t} - \frac{\gamma}{2}\alpha_j(t), \tag{A1}$$

$$\dot{\beta}_k(t) = -i\sum_{j=1}^{N_a} g_k^* e^{-ikr_j}\alpha_j(t)e^{i\delta\omega_k t}, \tag{A2}$$

where the detuning $\delta\omega_k = (|k| - k_a)v_g$. For the left propagation modes, we have $k < 0$, while for the right propagation modes, we have $k > 0$.

By integrating Eq. (A2) we have

$$\beta_k(t) = \beta_k(0) - i\sum_{j=1}^{N_a} g_k^* e^{-ikr_j}\int_0^t \alpha_j(t')e^{i\delta\omega_k t'}dt', \tag{A3}$$

where $\beta_k(0)$ is the photon amplitude at $t = 0$. On inserting Eq. (A3) into Eq. (A1) we can obtain

$$\begin{aligned}\dot{\alpha}_j(t) = &-i\sum_k g_k e^{ikr_j}\beta_k(0)e^{-i\delta\omega_k t} - \frac{\gamma}{2}\alpha_j \\ &- \sum_{l=1}^{N_a}\sum_k |g_k|^2 e^{-ik(r_j - r_l)}\int_0^\infty \alpha_l(t')e^{i\delta\omega_k t'}dt'e^{-i\delta\omega_k t},\end{aligned} \tag{A4}$$

where the first term on the right-hand side is the excitation by the input photon, the second term is the decay to the nonguided modes, and the third term is the interaction between the atoms induced by the guided photon modes.

For a long 1D waveguide we can replace the summation over k by an integration

$$\sum_k \to \frac{L_q}{2\pi}\int_{-\infty}^{\infty} dk, \tag{A5}$$

where L_q is the quantization length in the propagation direction. The summation over k in the third term of Eq. (A4)

can be calculated as

$$\sum_k |g_k|^2 e^{-ik(r_j-r_l)} e^{i\delta\omega_k(t'-t)} = \frac{L}{2\pi}\int_{-\infty}^{\infty} |g_k|^2 e^{-ik(r_j-r_l)} e^{i\delta\omega_k(t'-t)} dk \tag{A6}$$

$$\simeq \frac{L_q}{2\pi}|g_{k_a}|^2\left[\int_0^{\infty} e^{-ik(r_j-r_l)} e^{i(k-k_a)v_g(t'-t)} dk + \int_{-\infty}^{0} e^{-ik(r_j-r_l)} e^{i(-k-k_a)v_g(t'-t)} dk\right] \tag{A7}$$

$$= \frac{L_q}{2\pi}|g_{k_a}|^2\left\{e^{-ik_a(r_j-r_l)}\int_0^{\infty} e^{-i(k-k_a)[(r_j-r_l)-v_g(t'-t)]} dk + e^{ik_a(r_j-r_l)}\int_0^{\infty} e^{i(-k-k_a)[(r_j-r_l)+v_g(t'-t)]} dk\right\} \tag{A8}$$

$$\simeq \frac{L_q}{2\pi}|g_{k_a}|^2\left\{e^{-ik_a(r_j-r_l)}\int_{-\infty}^{\infty} e^{-i(k-k_a)[(r_j-r_l)-v_g(t'-t)]} dk + e^{ik_a(r_j-r_l)}\int_{-\infty}^{\infty} e^{i(-k-k_a)[(r_j-r_l)+v_g(t'-t)]} dk\right\} \tag{A9}$$

$$= L_q|g_{k_a}|^2\{e^{-ik_a(r_j-r_l)}\delta[(r_j-r_l)-v_g(t'-t)] + e^{ik_a(r_j-r_l)}\delta[(r_j-r_l)+v_g(t'-t)]\} \tag{A10}$$

$$= \frac{L_q|g_{k_a}|^2}{v_g}\left\{e^{-ik_a(r_j-r_l)}\delta\left[t'-\left(t+\frac{r_j-r_l}{v_g}\right)\right] + e^{ik_a(r_j-r_l)}\delta\left[t'-\left(t-\frac{r_j-r_l}{v_g}\right)\right]\right\} \tag{A11}$$

$$= \frac{\Gamma}{2}e^{ik_a|r_j-r_l|}\delta\left[t'-\left(t-\frac{|r_j-r_l|}{v_g}\right)\right], \tag{A12}$$

where $\Gamma = 2L_q|g_{k_a}|^2/v_g$. From Eq. (A6) to Eq. (A7) we rewrite the integration into the left-propagation and right-propagation parts and assume that the coupling strength is uniform for the modes close to k_a. From Eq. (A8) to Eq. (A9), for $k_a \gg 0$ we can extend the integration from 0 to $\pm\infty$ and use the identity $\int_{-\infty}^{\infty} e^{ikx}dx = 2\pi\delta(x)$. In Eq. (A11), since $t' \leqslant t$, when $r_j > r_l$ only the second term survives. On the contrary, when $r_j < r_l$ only the first term survives. Therefore, Eq. (A11) can be rewritten as Eq. (A12). By inserting Eq. (A12) into Eq. (A4) we can obtain Eq. (3) in Sec. II.

[1] J. M. Raimond, M. Brune, and S. Haroche, Rev. Mod. Phys. **73**, 565 (2001).
[2] M. Pelton, C. Santori, J. Vucković, B. Zhang, G. S. Solomon, J. Plant, and Y. Yamamoto, Phys. Rev. Lett. **89**, 233602 (2002),
[3] T. Wilk, S. C. Webster, A. Kuhn, and G. Rempe, Science **317**, 488 (2007).
[4] J. Hwang, M. Pototschnig, R. Lettow, G. Zumofen, A. Renn, S. Götzinger, and V. Sandoghdar, Nature (London) **460**, 76 (2009).
[5] P. Bermel, A. Rodriguez, S. G. Johnson, J. D. Joannopoulos, and Marin Soljacić, Phys. Rev. A **74**, 043818 (2006).
[6] E. M. Purcell, Phys. Rev. **69**, 37 (1946).
[7] M. D. Leistikow, A. P. Mosk, E. Yeganegi, S. R. Huisman, A. Lagendijk, and W. L. Vos, Phys. Rev. Lett. **107**, 193903 (2011).
[8] S. Noda, M. Fujita, and T. Asano, Nat. Photon. **1**, 449 (2007).
[9] V. M. Menon, W. Tong, F. Xia, C. Li, and S. R. Forrest, Opt. Lett. **29**, 513 (2004).
[10] Y. Shen, M. Bradford, and J.-T. Shen, Phys. Rev. Lett. **107**, 173902 (2011).
[11] Z. H. Wang, L. Zhou, Y. Li, and C. P. Sun, Phys. Rev. A **89**, 053813 (2014).
[12] M. Bradford, K. C. Obi, and J.-T. Shen, Phys. Rev. Lett. **108**, 103902 (2012).
[13] W.-B. Yan, J.-F. Huang, and H. Fan, Sci. Rep. **3**, 3555 (2013).
[14] M. Bradford and J.-T. Shen, Phys. Rev. A **85**, 043814 (2012).
[15] D. E. Chang, A. S. Sørensen, E. A. Demler, and M. D. Lukin, Nat. Phys. **3**, 807 (2007).
[16] D. Witthaut and A. S. Sorensen, New J. Phys. **12**, 043052 (2010).
[17] W.-B. Yan and H. Fan, Sci. Rep. **4**, 4820 (2014).
[18] H. Zheng, D. J. Gauthier, and H. U. Baranger, Phys. Rev. Lett. **111**, 090502 (2013).
[19] F. Ciccarello, D. E. Browne, L. C. Kwek, H. Schomerus, M. Zarcone, and S. Bose, Phys. Rev. A **85**, 050305(R) (2012).
[20] B. Dayan, A. S. Parkins, Takao Aoki, E. P. Ostby, K. J. Vahala, and H. J. Kimble, Science **319**, 1062 (2008).
[21] D. Englund, A. Faraon, B. Zhang, Y. Yamamoto, and J. Vučković, Opt. Exp. **15**, 5550 (2007).
[22] A. V. Akimov, A. Mukherjee, C. L. Yu, D. E. Chang, A. S. Zibrov, P. R. Hemmer, H. Park, and M. D. Lukin, Nature (London) **450**, 402 (2007).
[23] A. Wallraff, D. I. Schuster, A. Blais, L. Frunzio, R.-S. Huang, J. Majer, S. Kumar, S. M. Girvin, and R. J. Schoelkopf, Nature (London) **431**, 162 (2004).
[24] A. A. Abdumalikov Jr., O. Astafiev, A. M. Zagoskin, Yu. A. Pashkin, Y. Nakamura, and J. S. Tsai, Phys. Rev. Lett. **104**, 193601 (2010).
[25] I.-C. Hoi, C. M. Wilson, G. Johansson, T. Palomaki, B. Peropadre, and P. Delsing, Phys. Rev. Lett. **107**, 073601 (2011).
[26] I.-C. Hoi, T. Palomaki, J. Lindkvist, G. Johansson, P. Delsing, and C. M. Wilson, Phys. Rev. Lett. **108**, 263601 (2012).
[27] A. F. van Loo, A. Fedorov, K. Lalumiére, B. C. Sanders, A. Blais, and A. Wallraff, Science **342**, 1494 (2013).
[28] J.-T. Shen and S. Fan, Optics Lett. **30**, 2001 (2005).
[29] J.-T. Shen and S. Fan, Phys. Rev. Lett. **95**, 213001 (2005).
[30] F. Le Kien, S. Dutta Gupta, K. P. Nayak, and K. Hakuta, Phys. Rev. A **72**, 063815 (2005).
[31] J.-T. Shen and S. Fan, Phys. Rev. Lett. **98**, 153003 (2007).
[32] T. S. Tsoi and C. K. Law, Phys. Rev. A **80**, 033823 (2009).
[33] E. Rephaeli, J.-T. Shen, and S. Fan, Phys. Rev. A **82**, 033804 (2010).
[34] D. Roy, Phys. Rev. Lett. **106**, 053601 (2011).

[35] Y. Chen, M. Wubs, J. Mørk, and A. F. Koenderink, New J. Phys. **13**, 103010 (2011).
[36] B. Q. Baragiola, R. L. Cook, A. M. Brańczyk, and J. Combes, Phys. Rev. A **86**, 013811 (2012).
[37] K. Lalumière, B. C. Sanders, A. F. van Loo, A. Fedorov, A. Wallraff, and A. Blais, Phys. Rev. A **88**, 043806 (2013).
[38] S. Fan, S. E. Kocabas, and J.-T. Shen, Phys. Rev. A **82**, 063821 (2010).
[39] H. Zheng, D. J. Gauthier, and H. U. Baranger, Phys. Rev. A **82**, 063816 (2010).
[40] T. Shi and C. P. Sun, Phys. Rev. B **79**, 205111 (2009).
[41] V. I. Yudson and P. Reineker, Phys. Rev. A **78**, 052713 (2008).
[42] S. Xu and S. Fan, Phys. Rev. A **91**, 043845 (2015).
[43] Z. Liao, X. Zeng, S.-Y. Zhu, and M. S. Zubairy, Phys. Rev. A **92**, 023806 (2015).
[44] E. Vetsch, D. Reitz, G. Sague, R. Schmidt, S. T. Dawkins, and A. Rauschenbeutel, Phys. Rev. Lett. **104**, 203603 (2010).
[45] M. Bajcsy, S. Hofferberth, V. Balic, T. Peyronel, M. Hafezi, A. S. Zibrov, V. Vuletic, and M. D. Lukin, Phys. Rev. Lett. **102**, 203902 (2009).
[46] T. M. Babinec, J. M. Hausmann, M. Khan, Y. Zhang, J. R. Maze, P. R. Hemmer, and M. Lončar, Nat. Nanotechnol. **5**, 195 (2010).
[47] O. V. Astafiev, A. A. Abdumalikov, Jr., A. M. Zagoskin, Y. A. Pashkin, Y. Nakamura, and J. S. Tsai, Phys. Rev. Lett. **104**, 183603 (2010).
[48] J. Bleuse, J. Claudon, M. Creasey, N. S. Malik, J.-M. Gérard, I. Maksymov, J.-P. Hugonin, and P. Lalanne, Phys. Rev. Lett. **106**, 103601 (2011).
[49] A. Laucht, S. Pütz, T. Günthner, N. Hauke, R. Saive, S. Frédérick, M. Bichler, M.-C. Amann, A. W. Holleitner, M. Kaniber, and J. J. Finley, Phys. Rev. X **2**, 011014 (2012).
[50] O. Astafiev, A. M. Zagoskin, A. A. Abdumalikov Jr., Yu. A. Pashkin, T. Yamamoto, K. Inomata, Y. Nakamura, and J. S. Tsai, Science **327**, 840 (2010).
[51] L. Zhou, H. Dong, Y.-X. Liu, C. P. Sun, and F. Nori, Phys. Rev. A **78**, 063827 (2008).
[52] D. E. Chang, L. Jiang, A. V. Gorshkov, and H. J. Kimble, New J. Phys. **14**, 063003 (2012).
[53] H. Zheng and H. U. Baranger, Phys. Rev. Lett. **110**, 113601 (2013).
[54] S. Das, G. S. Agarwal, and M. O. Scully, Phys. Rev. Lett. **101**, 153601 (2008).
[55] U. Fano, Phys. Rev. **124**, 1866 (1961).
[56] S.-Y. Zhu and M. O. Scully, Phys. Rev. Lett. **76**, 388 (1996).
[57] S. Fan and J. D. Joannopoulos, Phys. Rev. B **65**, 235112 (2002).
[58] A. B. Khanikaev, C. Wu, and G. Shvets, Nanophotonics **2**, 247 (2013).
[59] R. H. Dicke, Phys. Rev. **93**, 99 (1954).
[60] M. G. Benedict, A. M. Ermolaev, V. A. Malyshev, I. V. Sokolov, and E. D. Trifonov, *Super-Radiance Multiatomic Coherent Emission* (Institute of Physics, Philadelphia, 1996).
[61] S. T. Cundiff and J. Ye, Rev. Mod. Phys. **75**, 325 (2003).
[62] J. Ye, L. S. Ma, T. Daly, and J. L. Hall, Opt. Lett. **22**, 301 (1997).
[63] D. J. Jones, S. A. Diddams1, J. K. Ranka, A. Stentz, R. S. Windeler, J. L. Hall, and S. T. Cundiff, Science **288**, 635 (2000).
[64] D. K. Armani, T. J. Kippenberg, S. M. Spillane, and K. J. Vahala, Nature (London) **421**, 925 (2003).
[65] T. J. Kippenberg, S. M. Spillane, and K. J. Vahala, Phys. Rev. Lett. **93**, 083904 (2004).
[66] P. Del'Haye, A. Schliesser, O. Arcizet, T. Wilken, R. Holzwarth, and T. J. Kippenberg, Nature (London) **450**, 1214 (2007).
[67] C. Ren and H. F. Hofmann, Phys. Rev. A **89**, 053823 (2014).
[68] M. O. Scully and M. S. Zubairy, *Quantum Optics* (Cambridge University Press, New York, 2001).
[69] J.-T. Shen and S. Fan, Phys. Rev. A **79**, 023837 (2009).
[70] Z. Liao and M. S. Zubairy, Phys. Rev. A **90**, 053805 (2014).